

# Landslide susceptibility modelling applying user-defined weighting and data-driven statistical techniques in Cox's Bazar Municipality, Bangladesh

Bayes Ahmed<sup>1</sup> 

Received: 1 April 2015 / Accepted: 27 July 2015 / Published online: 1 August 2015  
© Springer Science+Business Media Dordrecht 2015

**Abstract** Landslides are common geophysical hazards in the highly urbanized hilly areas of Cox's Bazar Municipality, Bangladesh. Every year, during the monsoon, landslides cause human casualties, property damage, and economic losses. Indiscriminate hill cutting, developing settlements in dangerous hill slopes, and torrential rainfall in short period of time are responsible for triggering landslide disasters. The aim of this paper is to produce landslide susceptibility maps (LSM) to help reduce the risks of landslides. Geographic information system and remote sensing-based techniques were used for LSM considering 12 relevant factor maps (i.e. slope, land cover, NDVI, geology, geomorphology, soil moisture, rainfall pattern, distance from road, drain, stream, structure, and faults—lineaments). For the modelling purpose, four techniques were implemented—artificial hierarchy process (AHP), weighted linear combination (WLC), logistic regression (LR), and multiple logistic regression (MLR). A landslide inventory map with 74 historical landslide locations was prepared by field surveying. The modelling results are validated using the area under the relative operating characteristics curves (AUC). AUC values of AHP, WLC, LR, and MLR methods are calculated as 88, 85.90, 74.90, and 90.40 %, respectively.

**Keywords** Landslide susceptibility mapping · Logistic regression · Artificial hierarchy process · Weighted linear combination · ROC curve · GIS

## 1 Introduction

Landslide hazards are a common threat for the vulnerable people living in the urbanized hilly slopes of Cox's Bazar Municipality (CBM), Bangladesh. The first fatal landslide event (caused six casualties) in CBM was recorded on 16 June 2003. A series of other rainfall-triggered landslides caused at least 47 human casualties in CBM on 15 June 2010

---

✉ Bayes Ahmed  
bayes.ahmed.13@ucl.ac.uk; bayesahmed@gmail.com

<sup>1</sup> Institute for Risk and Disaster Reduction, Department of Earth Sciences, University College London (UCL), Gower Street, London WC1E 6BT, UK

(CDMP-II 2012: 12). Moreover, recently 5 days (from 23 to 27 June 2015) of continuous rainfall (about 1070 mm) and concurrent landslides in Cox's Bazar district caused 15 casualties, more than 100 villages were flooded, 1000 houses destroyed, and roads damaged. This is how every year during the monsoon period, landslide hazards are continuing to cause human casualties, injuries, and property damage in CBM. Moreover, the severity of the landslide disaster is intensifying gradually. This is happening because of increase in urban population, indiscriminate hill cutting, inappropriate agricultural practice, unplanned city planning, development of unauthorized settlements in steep slopes, not incorporating the indigenous cultural knowledge in hill management, and lack of institutional capabilities to reduce the community vulnerability. At this drawback, the main objective of this article is to prepare the landslide susceptibility maps to help reducing the risks of landslide disasters in CBM.

## 2 Study area profile

CBM is located in Cox's Bazar District (CBD) that is one of the five districts of the south-eastern Chittagong Hill Tracts (CHT) region (Fig. 1a). The study area, CBM, is approximately situated within  $22^{\circ}23'30''$  and  $22^{\circ}27'30''$  north latitude and between  $91^{\circ}58'$  and  $92^{\circ}2'$  east longitude (Fig. 1b). It is bounded on the west by the Bay of Bengal, on the northeast by *Bakkhali* River, and on the north by *Moheshkhali* Channel (Fig. 1b). The total area of CBM is about 20.78 sq.km. The population of CBM increased fourfold in the past two decades (1991–2011), which is now around 1,67,477 (BBS 2013).

CBM is characterized by hills, sea beach, medium-to-low density forests, and staggering natural beauty. The world's longest uninterrupted natural sandy sea beach (about 120 km) is located in CBD (Hossain 2012). The major commercial part of the beach is covered by CBM; therefore, it has become the country's most attractive tourist spot. As a result of that, thousands of people are migrating in search of employment opportunities and the rate of urbanization is high in CBM. This is how the urban built-up area in CBM increased by approx. threefold (3.27–9.74 sq.km) from 1990 to 2015 (Fig. 2).

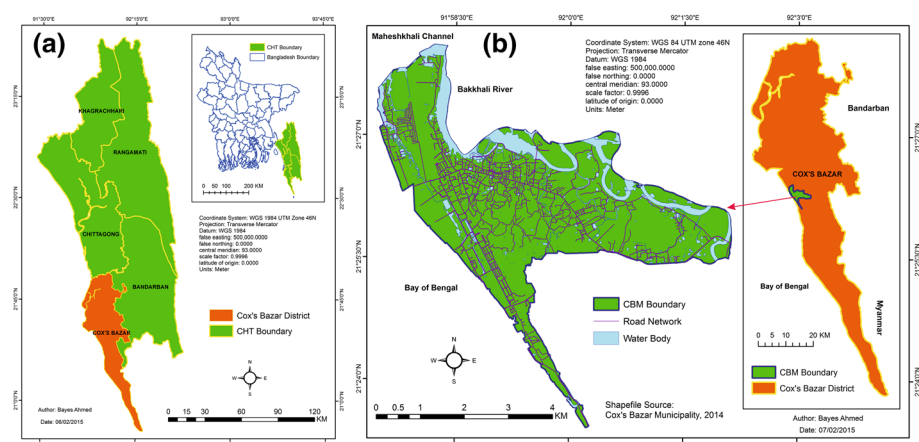


**Fig. 1** **a** Location of CBD in CHT and **b** location of the study area, CBM, in CBD

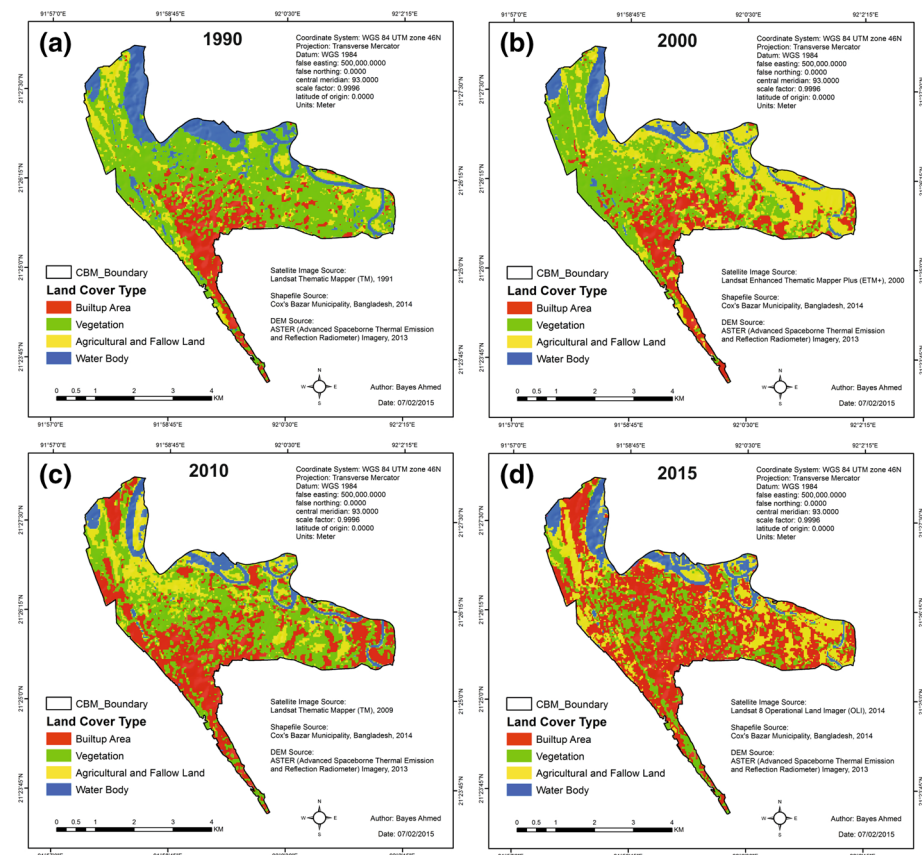


**Fig. 2** Land cover maps of CBM (1990–2015)

The arrival of large number of poor people from other parts of Bangladesh is evident in CBM. At the same time, the responsible authorities are failing to offer them cheap accommodation and other necessary facilities. Therefore, the disadvantaged people are illegally cutting the hills for the development of new settlements (Fig. 3), and making themselves more vulnerable to landslide hazards. In recent years, the most devastating landslides took place due to hill cutting, deforestation, and torrential rainfall (CDMP-II 2012: 12). These are the root causes of landslide disasters in CBM.

## 2.1 Physiographic and geological features

CBM is located on the north-eastern part of the Inani Anticline. Inani is a narrow and elongated structure in which the Tipam Sandstone formation is characterized by steep zone. It is represented by NNW–SSE trending low hillocks attaining maximum elevation of 54.86 m. CBD includes two distinct geological settings, namely tertiary folded belt and coastal deposits. The tertiary folded belt extends north–south that is characterized by long narrow folds. The coastal Holocene deposits overlie with the tertiary rocks, resulting in different surficial forms. The tertiary hills represent the geological structures of CBM.

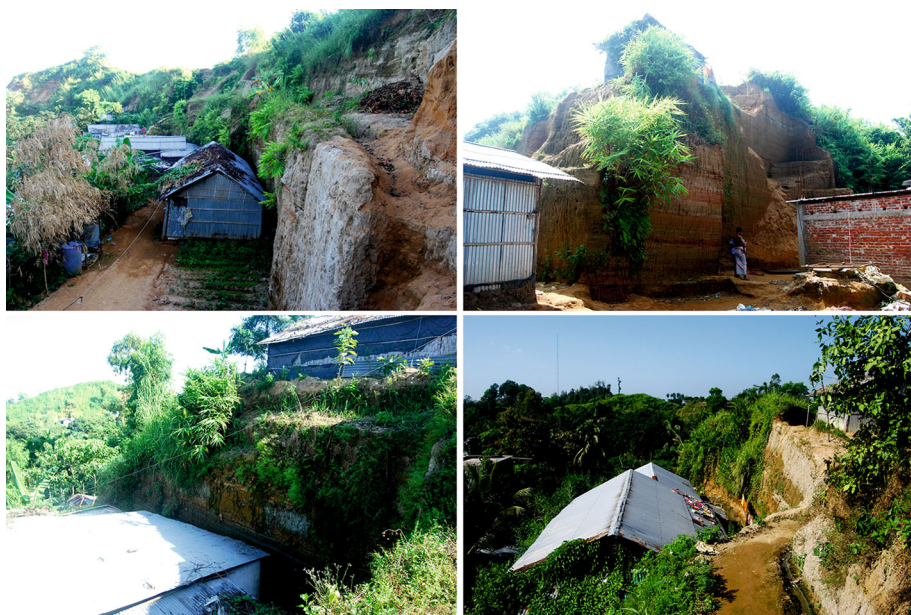


**Fig. 3** Development of human settlements by illegal and indiscriminate hill cutting in CBM. *Source:* Bayes Ahmed, Field Survey, July–October 2014

CBM and its surroundings predominantly consist of Dihing formation and Dupi Tila formation of Plio-Pleistocene age. The formations are characterized by fine- to medium-grained poorly consolidated sandstone and clayey sandstone of variable colours ranging from yellow, brown to grey (CDMP-II 2012: 28–30).

The Cox's Bazar cliff runs from NNW to SSE direction along the shore of the Bay of Bengal. The range lies on the eastern side of the Bay of Bengal. The beach runs approximately along S35°E. Eastern side of the cliff is accompanied by a series of hills. The highest ridge of the Cox's Bazar hill is about 82 m above the sea level. Valleys are irregularly situated in this hill range. The height of the cliff along the beach varies within a narrow range from about 50 to 82 m, and these cliffs terminate abruptly against the beach (CDMP-II 2012: 18).

It is believed that the present-day morphology of the area is influenced by the Holocene sea level rise, and tidal and fluvial discharges. The mountain forming bedrock of the escarpment, from where the landslide occurs, is mainly formed with two lithological units: bluish grey thinly laminated shale unit, and yellowish brown cross-bedded to massive medium- to fine-grained sandstone. Sandstones are comparatively loose and less compact, and the top part of this unit is highly weathered. The failed mass comprised of highly weathered rock and moderately weathered rock. After the slides at places, a moderately weathered rock is exposed. The exposed rock units are mostly composed of light brown fine- to medium-grained sand, silt, and clay (CDMP-II 2012: 46).

## 2.2 Rainfall pattern

As the landslide hazards in CBM are rainfall induced, it is important to analyse the rainfall pattern. To conduct the analysis, the daily precipitation data (1950–2013) of CBD is

collected from the Bangladesh meteorological department. The rainfall pattern is analysed using ‘RClimDex’, which runs on ‘R’ statistical software and is maintained by the Climate Research Branch of Meteorological Service of Canada (Zhang and Yang 2004).

A total of seven precipitation indices (Zhang and Yang 2004) are calculated (Table 1) that are related to landslide hazards in CBM: monthly maximum 1-day precipitation ( $Rx1\text{ day}$ ); monthly maximum consecutive 5-day precipitation ( $Rx5\text{ day}$ ); annual count of days when precipitation  $>10\text{ mm}$  ( $R10$ ), precipitation  $>20\text{ mm}$  ( $R20$ ) and precipitation  $>50\text{ mm}$  ( $R50$ ); maximum number of consecutive wet days (CWD); and annual total wet day precipitation (PRCPTOT).

The results show (Table 1) that CBM has an average annual precipitation of 3750 mm with a high increasing trend of 4.56 % (Fig. 4). Moreover, the monthly maximum 1 and 5

**Table 1** Rainfall pattern analysis of Cox’s Bazar district (1950–2013)

Precipitation index (unit)	Trend of rainfall indices			Rainfall pattern		
	Slope	Slope error	P value	Min.	Max.	Avg.
$Rx1\text{ (mm)}$	0.461	0.618	0.459	130	720	217
$Rx5\text{ (mm)}$	0.633	0.781	0.421	303	880	533
$R10\text{ (days)}$	0.118	0.056	0.039	50	90	76
$R20\text{ (days)}$	0.088	0.050	0.082	32	68	54
$R50\text{ (days)}$	0.056	0.030	0.070	13	33	25
CWD (days)	-0.046	0.045	0.318	8	35	21
PRCPTOT (mm)	4.561	3.781	0.233	2128	4988	3750

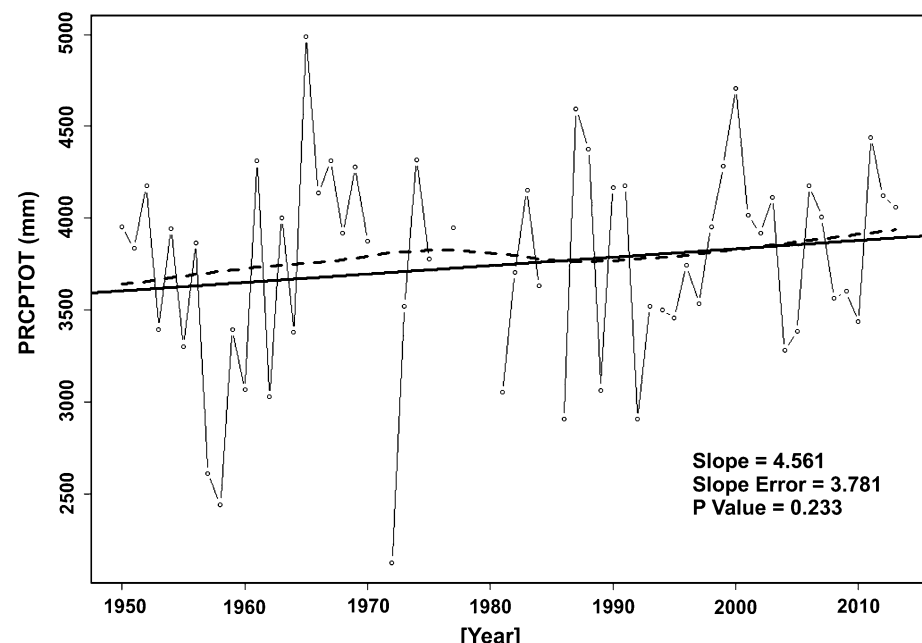


**Fig. 4** Annual total precipitation in wet days (precipitation  $\geq 1\text{ mm}$ ) in CBD

consecutive days precipitation, number of heavy ( $\text{PRCP} \geq 10 \text{ mm}$ ) and very heavy rainfall days ( $\text{PRCP} \geq 20 \text{ mm}$ , and  $\text{PRCP} \geq 50 \text{ mm}$ ) indices are also showing gradual upward trend (Table 1; Fig. 5).

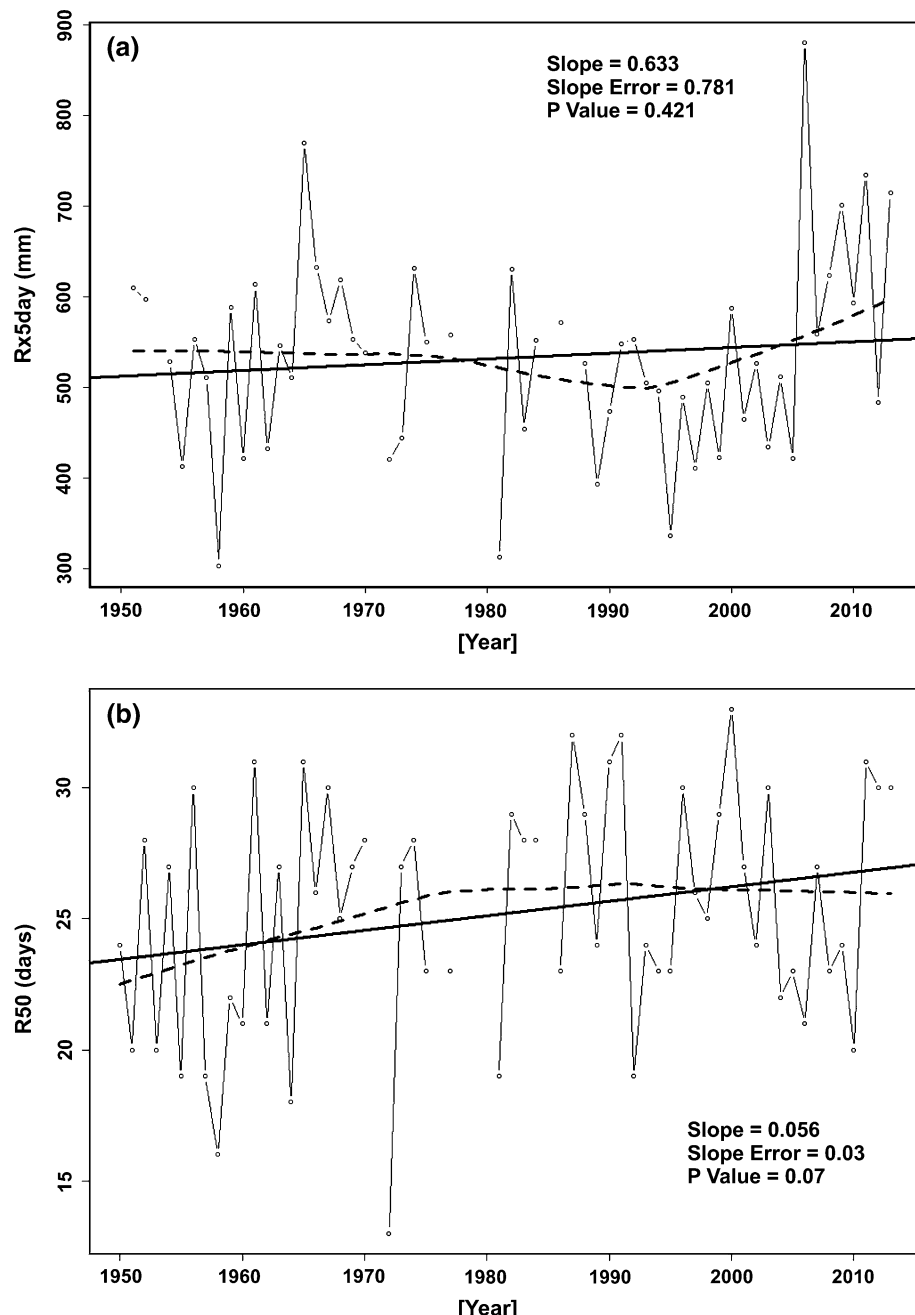


**Fig. 5** **a** Rx5 day and **b** R50 precipitation index graphs of CBD

It is estimated that around 96 mm rainfall in 24 h or 185 mm rainfall in 48 h can cause a landslide in Cox's Bazar (CDMP-II 2012: 103). CBM is likely to have 21 consecutive days of precipitation and hit by heavy rainfall ( $\geq 50$  mm) for a total of 25 days during the rainy season (Table 1). The monthly five consecutive days of precipitation in monsoon is calculated as 533 mm (Table 1), which is much greater than the landslide early-warning threshold of 200 mm (CDMP-II 2012). The patterns suggest that the gradual increasing trend of rainfall indices can worsen the landslide disaster scenario in CBM.

### 2.3 Landslide mechanism

The recent history shows that the excessive rainfall is the main triggering factor of the slides. The escarpment has three well-developed joint systems—one is parallel to bedding plane, and the other two are vertical and almost perpendicular to each other. The joints are filled with fine clayey material. During the rainy season, the clay-filled joints get saturated. Then, extrusion of joints takes place by opening up and widening the joints. During the dry season, the water-saturated joints become dry and shrink in volume. It reduces the cohesive strength and bonding. This phenomenon is repeated several times during dry and wet periods until it breaks down from the main mass due to the combined effect of the gravity and loss of cohesion (CDMP-II 2012: 73).

## 3 Literature review

Landslide is a movement of mass of soil (earth or debris) or rock down a slope (Cruden 1991). Landslide disaster is defined as serious disruption of the functioning of a community or a society causing widespread human, material, economic, or environmental losses that exceed the ability of the affected community or society to cope using its own resources (Couture 2011). According to the world disasters report 2014, a total of 173 landslide disasters were reported worldwide (2004–2013) causing about 8739 human casualties and affecting 3.2 million people. Among the 173 landslides worldwide (2004–2013), a total of 115 events occurred only in Asia that caused approximately 7098 deaths and affecting 3 million people (Ahmed et al. 2014; IFRC 2014). Moreover, the recent earthquakes in Nepal (25 April 2015) generated around 3000 landslides and other mass movements (ICIMOD 2015). Therefore, it can be stated that people living in the mountainous or hilly slopes in Southeast Asia region are highly vulnerable to landslide hazards.

It is argued that the studies of disaster essentially begin with the attempts to understand the hazard and its impact. Alexander (2006) stated that vulnerability is a greater determinant of disaster risk than hazards themselves. The recent works on disaster risk reduction science are emphasizing more on vulnerability studies (Alexander 2014: 212; Birkmann 2006; Alexander 2004; Wisner et al. 2004: 10). But dealing with hazard issues is also important. It is true that the existence of a group of socially, economically, and culturally vulnerable people can also be responsible for the disaster itself. But if the vulnerable communities have no idea on the frequency, magnitude, intensity, and nature of the particular hazard, then the situation can be worse. In this regard, producing the susceptibility maps for landslide hazards can be the first step for reducing the associated risks.

Rainfall-induced landslides in the urbanized hilly areas are being considered as an emerging disaster in Bangladesh. The human casualties, property damage, and economic loss associated with landslide hazards are gradually increasing in CHT region (Ahmed and

Rubel 2013). But in case of urban landslides, it is argued that the susceptibility terrain can be mapped easily, and the occurrences can be forecast in real time (Alexander 1991). Therefore, it is essential to produce landslide susceptibility maps (LSM) and integrate it to support land management decision-making for generating community safety (Akgun 2012).

Recently, the geographic information system (GIS) and remote sensing (RS) techniques are being popular in mapping the areas susceptible to landslides. These techniques are being frequently used for landslide hazard assessment, vulnerability and risk mapping, and disaster management for landslides (Kavzoglu et al. 2014; Talaei 2014). For example, Lee and Lee (2006), Reis et al. (2012), and Lee and Sambath (2006) have used frequency ratio probabilistic model to predict the landslide locations. Pellicani et al. (2013), Park et al. (2013), and Feizizadeh and Blaschke (2013) implemented the Analytic Hierarchy Process (AHP) to produce LSM. Reis et al. (2012), Lee and Sambath (2006), Kavzoglu et al. (2014), Park et al. (2013), Talaei (2014), and Lee (2004) implemented the logistic regression model for LSM.

Some other techniques for LSM are also being implemented by the researchers such as geographically weighted principal component analysis (Sabokbar et al. 2014; Sujatha and Rajamanickam 2011), likelihood ratio model (Lee 2004), fractal method (Li et al. 2012), support vector machine (Ballabio and Sterlacchini 2012; Kavzoglu et al. 2014), multiple logistic regressions (Ohlmacher and Davis 2003; Ahmed and Rubel 2013), weighted linear combination (Kavzoglu et al. 2014; Feizizadeh and Blaschke 2013), weight of evidence method (Kayastha et al. 2012; Yilmaz et al. 2012; Armaş 2012), artificial neural network method (Park et al. 2013; Pradhan et al. 2010; Khamehchiyan et al. 2011), fuzzy logic (Kayastha et al. 2013), neuro-fuzzy model (Sezer et al. 2011; Oh and Pradhan 2011), and decision tree (Yeon et al. 2010) etc.

In broader sense, the landslide susceptible maps can be drawn using either qualitative or quantitative approaches (Guzzetti et al. 1999). Qualitative maps are produced by assigning weights to all the factor maps affecting landslide based on researchers' expertise, while the quantitative approaches involve techniques to analyse the relations between causes of landslides based on different probabilistic/statistical models. Both qualitative and quantitative methods take into consideration the relevant factors affecting landslides and areas where past landslides occurred (Park et al. 2013).

## 4 Data collection

The first step of LSM is identifying the causative factors of landslide hazards and then collecting/generating the relevant factors maps. For this research purpose, 12 factor maps and a landslide inventory map was produced. All the images were projected to the universal transverse Mercator (UTM) zone 46 North system, with the world geodetic system (WGS)-1984 Datum. Each image resolution was set to cell size of 30 × 30 m, with 268 columns and 290 rows.

### 4.1 Landslide inventory map

To prepare the landslide inventory map, extensive fieldwork was carried out in CBM from July to October 2014. A total of 74 landslides were identified in CBM (Fig. 6). A handheld global positioning system (GPS) device was used to identify the locations of the landslides

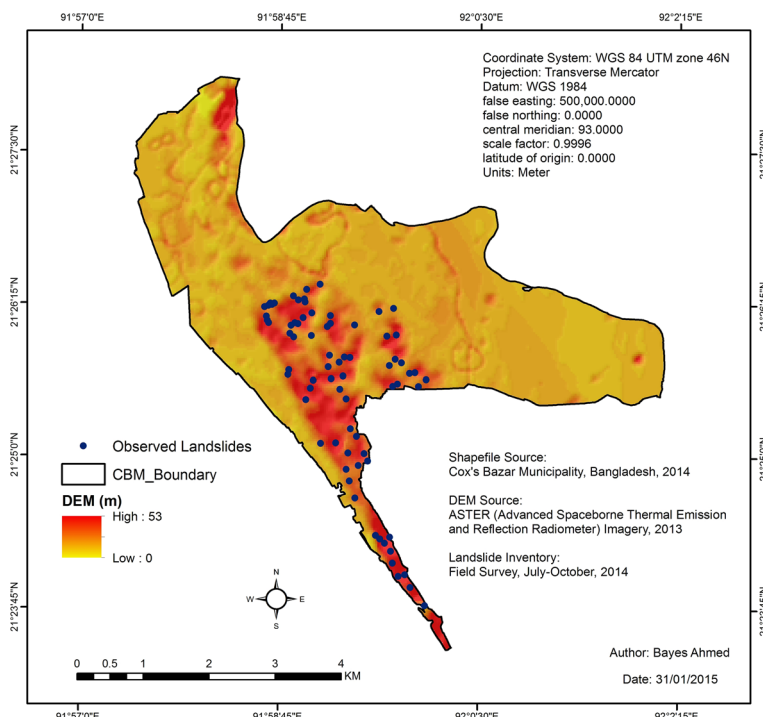


**Fig. 6** Landslide inventory map of CBM

through field surveying. For each landslide hazard location, information on the soil type, landslide width and length, slope angle, vegetation type, number of houses and population, and landslide occurrence history were collected. The digital elevation model (DEM) image, dated on 29 November 2013, was acquired from the advanced space-borne thermal emission and reflection radiometer (ASTER) global digital elevation model web-portal (Tachikawa et al. 2011).

#### 4.2 Land cover mapping

The land cover maps of CBM (1990, 2000, 2010, and 2015) were prepared using the maximum likelihood supervised classification technique (Ahmed 2011; Ahmed et al. 2013a). This technique is useful when the analyst has a priori knowledge on the study area (Ahmed and Ahmed 2012; Ahmed et al. 2013b). The relevant Landsat satellite images

**Table 2** Details of the landsat satellite images

Respective year	Date acquired	Sensor
1990	19 November 1991	Landsat 7 thematic mapper (TM)
2000	21 December 2000	Landsat 7 enhanced thematic mapper plus (ETM+)
2010	5 February 2009	Landsat 7 thematic mapper
2015	24 April 2014	Landsat 8 operational land imager (OLI)

**Table 3** Contents of different land cover types

Land cover type	Description
Built-up area	Urban and rural settlements, road and drainage network, pavements, man-made structures and infrastructure
Vegetation	Hill forest, mangrove plantation, rubber plantation, shrub land, grassland, and other natural vegetation
Agricultural and fallow land	Irrigated and rained herbaceous crops, crop in sloping lands, sea beach, bare soil, fallow land, sand fillings, open space, park etc.
Water body	Bay of Bengal, river, ponds, reservoirs, lake, canals, low land, and other temporary/permanent wetlands

(Table 2) were downloaded from the global visualization viewer of the United States Geological Survey (USGS 2015). CBM is located in Landsat path 136 and row 45. Then, four broad land cover classes (Table 3) were identified—builtup area, vegetation, agricultural and fallow land, and water body (Fig. 2).

After preparing the base maps (Fig. 2), it is important to assess the accuracies of the classified images generated from the satellite data sets. It was not possible to ground-truth all the classified images. Therefore, for conducting the accuracy assessment, a total of 200 reference pixels were generated for each base map using stratified random sampling method (Ahmed et al. 2013a). Then, the authentic base maps of CBM were collected from the Survey of Bangladesh, and the municipality office for comparison purpose. Historical Google Earth images were also used, and finally, GPS values were collected from field visits in CBM for comparing the base map of 2015. This is how the accuracy assessments were performed using ERDAS IMAGINE software. The producers, users, and overall accuracies of all the classified images were found to be greater than 85 %, which is acceptable for further analysis (Ahmed and Ahmed 2012; Ahmed et al. 2013a).

### 4.3 Precipitation map

The precipitation map of Bangladesh (Fig. 7a) is prepared using the collected daily precipitation data (1950–2010) for all the 35 rainfall stations. The average annual rainfall of Bangladesh is found ranging from 1480.68 to 4074.08 mm, and the range of monsoon rainfall (April–October) is calculated as 1400.39–3913.91 mm. Moreover, it is found that CBM falls in the high precipitation zone of Bangladesh, and the monsoon period covers about 96 % of the total annual rainfall. As all the landslides in CBM are rainfall induced (Ahmed and Rubel 2013), only the monsoon rainfall pattern is used for further analysis (Fig. 7b).

### 4.4 Normalized difference vegetation index

The Normalized Difference Vegetation Index (NDVI) is an indicator that represents the greenness—the relative density of vegetation. NDVI values range from +1.0 to −1.0. NDVI equation is as follows (ArcGIS 10.2 Help 2014):

$$\text{NDVI} = ((\text{IR} - R)/(\text{IR} + R)) \quad (1)$$

where IR = pixel values of infrared band and R = pixel values of red band. The higher NDVI value indicates higher density of vegetation and vice versa. Low NDVI values (<0.1) represent snow, sand, or rock; mid NDVI values (0.1–0.5) represent small trees, grasslands, and shrubs; while high NDVI values (>0.5) represent dense hill forests and

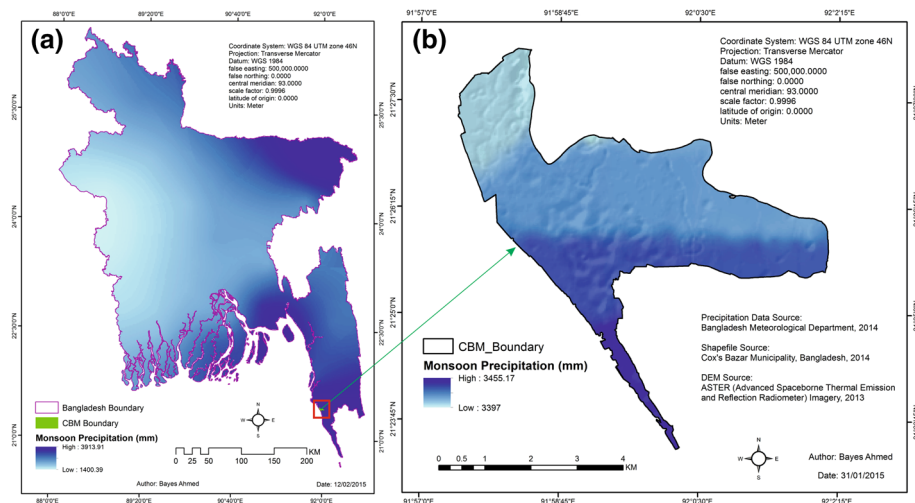


**Fig. 7** **a** Average annual precipitation of Bangladesh, **b** Average annual monsoon rainfall in CBM (1950–2010)

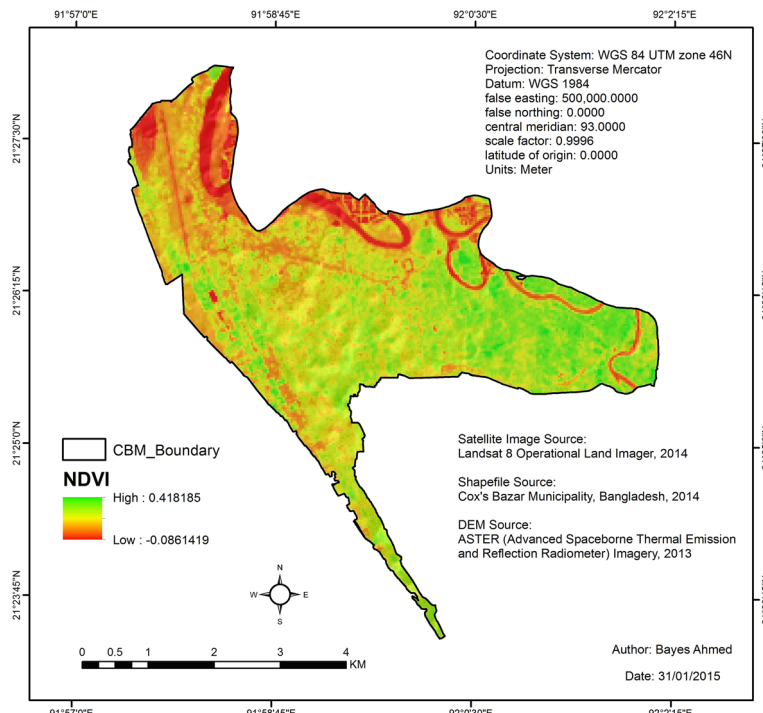


**Fig. 8** NDVI map of CBM

crops (ArcGIS 10.2 Help 2014). Landsat 8 OLI images (Table 2) were used for generating NDVI image of CBM (Fig. 8). In this case, band 5 and band 4 were considered as IR and *R*, respectively (USGS 2014).

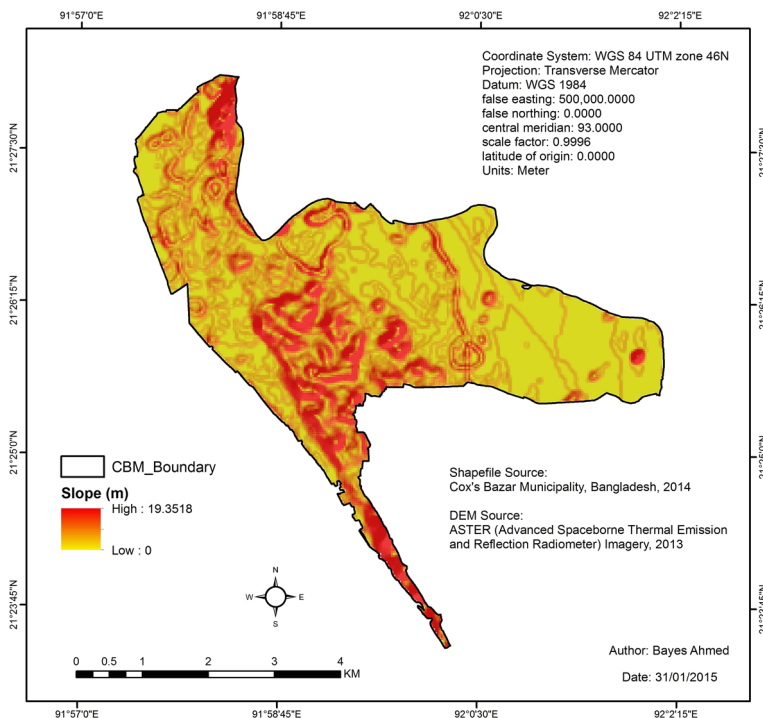


**Fig. 9** Slope map

#### 4.5 Other layers

The slope (Fig. 9) and stream network maps (Fig. 10) were generated from the DEM. The road (Fig. 11), drainage network (Fig. 12), and existing structure (Fig. 13) layers were collected from CBM. The geological (Fig. 14), geomorphological (Fig. 15), soil moisture (Fig. 16), and fault-lineaments (Fig. 17) layers were collected from the Geological Survey of Bangladesh. Euclidean distance technique was implemented to generate the distance images. This technique calculates the distance from each raster cell to its nearest source (ArcGIS 10.2 Help 2014).

### 5 Methodology

In this research, two user-defined weight-based qualitative (WLC, and AHP), and two data-driven statistical (logistic regression, and multiple logistic regression) techniques were chosen. These techniques are being widely used by the researchers for LSM (Ohlmacher and Davis 2003; Yilmaz et al. 2012; Park et al. 2013). SPSS 22, ArcGIS 10.2, and IDRISI Selva software were used for LSM.

#### 5.1 Analytical hierarchy process

AHP method, developed by Satty in the mid-1970s, is based on multi-criteria evaluation (MCE) techniques. AHP can be used for incorporating technological, economic, and socio-

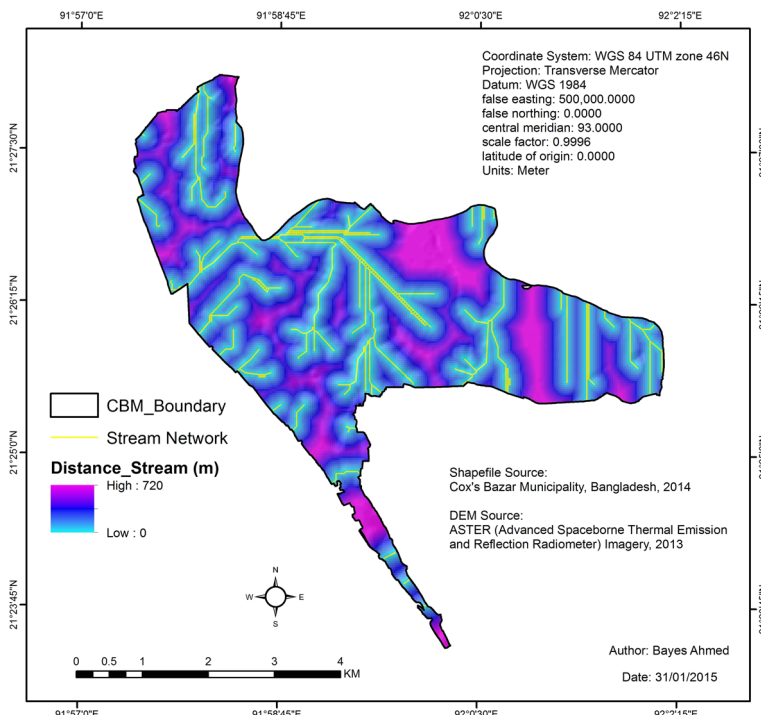


**Fig. 10** Distance from stream map

political issues (Saaty 1977; Park et al. 2013). AHP involves pairwise comparison of the factor maps or decision variables. Initially, each factor map is assigned with a weight against every other factor to construct a pairwise comparison matrix (Malczewski 2004). The weight rating follows a 9-point continuous scale: (1/9, 1/8, 1/7, 1/6, 1/5, 1/4, 1/3, 1/2, 1, 2, 3, 4, 5, 6, 7, 8, 9). Here, the factor weight values greater than 1 represent more importance, less than 1 represent less importance, and 1 represent equal importance in relation to another factor (Eastman 2012). The weights also undertake eigenvalues and eigenvectors calculations. If one factor has preference then its eigenvector component is larger than that of the other. The eigenvector values sum to unity (Reis et al. 2012). In AHP, an index of consistency to determine the degree of consistency, termed as the Consistency Ration (CR), is used that can be expressed as (Reis et al. 2012):

$$CR = CI/RI \quad (2)$$

where RI = mean/average consistency index, and CI = consistency index, which is as follows:

$$CI = (\lambda_{\max} - n)/(n - 1) \quad (3)$$

where  $\lambda_{\max}$  = largest eigenvector of the matrix, and  $n$  = the order of the matrix (Reis et al. 2012).

CR value above 0.1 indicates inconsistent factor ratings, and the model is discarded (Saaty 1977). In this case, the model needs necessary revisions of the factor weights.

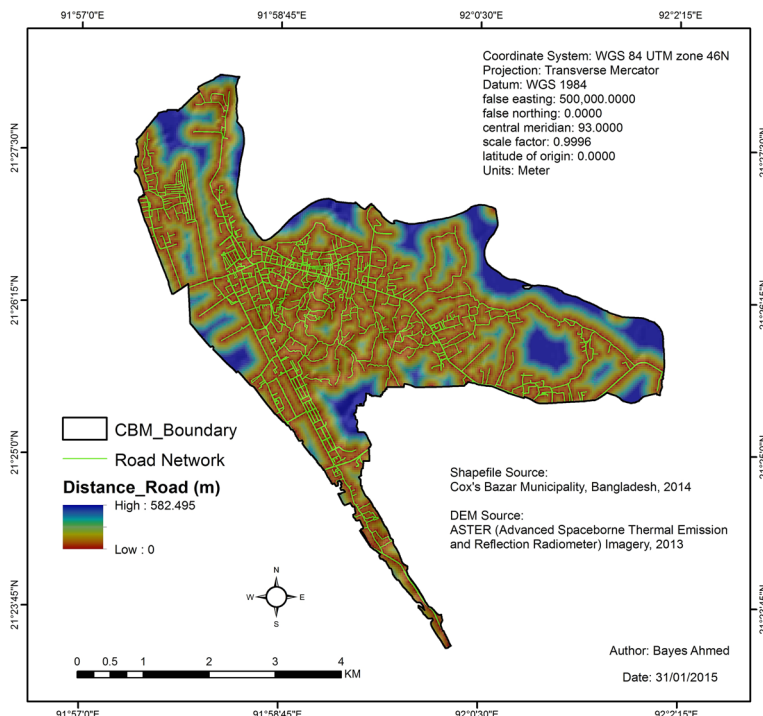


**Fig. 11** Distance from road

## 5.2 Weighted linear combination

WLC is a simple additive weighting method. In WLC, initially a weight is assigned to each factor. The researcher based on expert opinion and field experience determines the weights. The determined weights are used with their corresponding individual standardized criteria as input for the WLC aggregation method. A total weight is then obtained as a sum of the products of each criteria and its weight (Eastman 2012; Aydi et al. 2013):

$$S = \sum_{i=1}^n w_i x_i \quad (4)$$

where  $S$  = suitability index,  $w_1, w_2, \dots, w_n$  = the weights of the criteria, and  $x_1, x_2, \dots, x_n$  = the standardized score of the criteria. Moreover, as the sum of the weights is constrained to 1, the final combined estimate is presented on the same scale (Aydi et al. 2013).

## 5.3 Logistic regression

Logistic regression (LR) allows the analysis of binary outcomes such as 0 or 1, and it is determined from one or more independent factors (Dai and Lee 2002). LR produces the best fitting model to describe the relationship between the dependent (e.g. landslides) and independent variables (e.g. relevant factor maps). In this model, the dependent variable can have only two values: 1 (i.e. landslide exists) and 0 (i.e. landslide does not exist). LR does

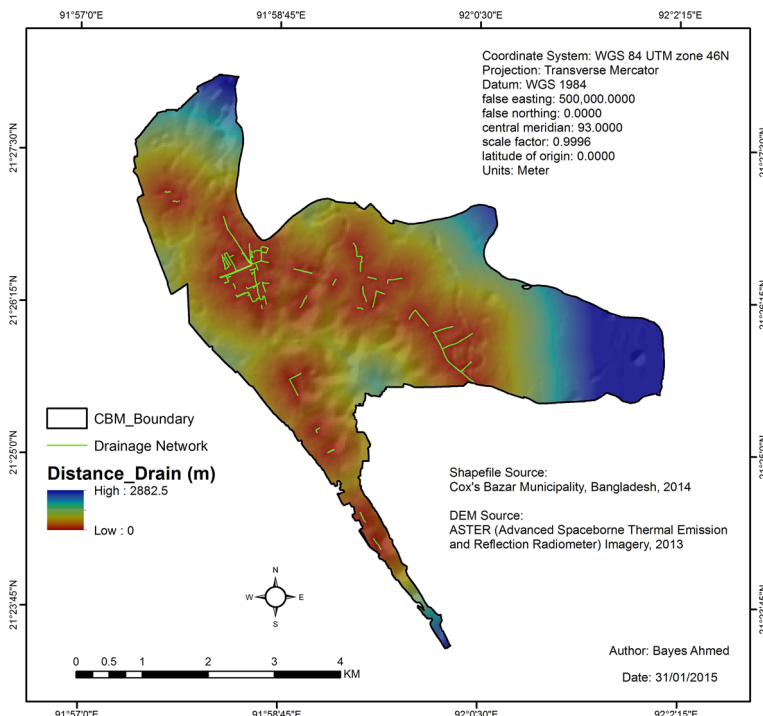


**Fig. 12** Distance from drain

not define susceptibility directly, but a surface interface can be produced using the probability. It can be described as follows (Ayalew and Yamagishi 2005):

$$Y = \text{Logit}(p) = \ln(p/(1-p)) = C_0 + C_1 X_1 + C_2 X_2 + \dots + C_n X_n \quad (5)$$

where  $p$  = the probability that the dependent variable ( $Y$ ) is 1,  $p/(1-p)$  = the likelihood ratio,  $C_0$  = the intercept, and  $C_1, C_2, \dots, C_n$  = coefficients, which measure the contribution of independent factors ( $X_1, X_2, \dots, X_n$ ) to the variations in  $Y$ . The goodness of fit in LR is calculated using Eq. 6 (Eastman 2012):

$$\text{Pseudo } R\text{-square} = 1 - (\log(\text{Likelihood})) / \log(L_0) \quad (6)$$

where Likelihood = the value of the likelihood function for the full model is fitted; and  $L_0$  = the value of the likelihood function if all coefficients except the intercept are 0.

Pseudo  $R$ -square 1 indicates perfect fit, 0 indicates no relationship, and greater than 0.2 is considered as a good fit (Eastman 2012).

#### 5.4 Multiple logistic regression

Multiple logistic regression (MLR) model considers multiple explanatory variables. In MLR, the landslide occurrence is expressed as a continuous variable (Ohlmacher and Davis 2003). The MLR model for the log odds is (Agresti 2007: 115):

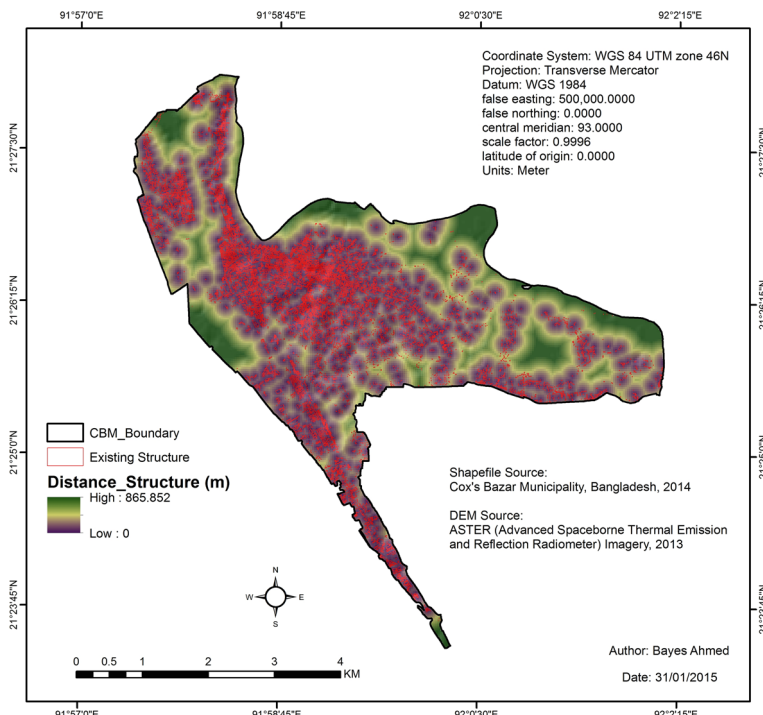


**Fig. 13** Distance from existing structures

$$\text{logit} [P(Y = 1)] = \alpha + \beta_1 x_1 + \beta_2 x_2 + \cdots + \beta_k x_k \quad (7)$$

where  $\beta_i$  refers to the effect of  $x_i$  on the log odds that  $Y = 1$ , controlling the other  $xs$ ; and  $k$ , predictors for a binary response  $Y$  by  $x_1, x_2, \dots, x_k$ .

The study area, CBM, is selected based on historical landslides and rainfall pattern. Then, extensive fieldwork was conducted to locate the landslides and analyse the landslide mechanism. After selecting the factor maps, different weight-based and statistical methods were implemented for producing LSM. Finally, the LSMs were validated for comparison purpose. The flow chart of methodology is illustrated in Fig. 18.

## 6 Results

### 6.1 AHP and WLC results

The first step of AHP method is to construct a pairwise comparison matrix for all the factors (Table 4). The factor weights were assigned based on the knowledge gathered from fieldwork in CBM such as expert opinion surveying, and community-based participatory rural appraisal (PRA) surveying. Initially several community-based vulnerability maps (Fig. 19) were produced using the PRA techniques.

The PRA vulnerability maps, as depicted in Fig. 19, helped to understand the community views on landslide risks and the priority of the relevant factors. This is how the

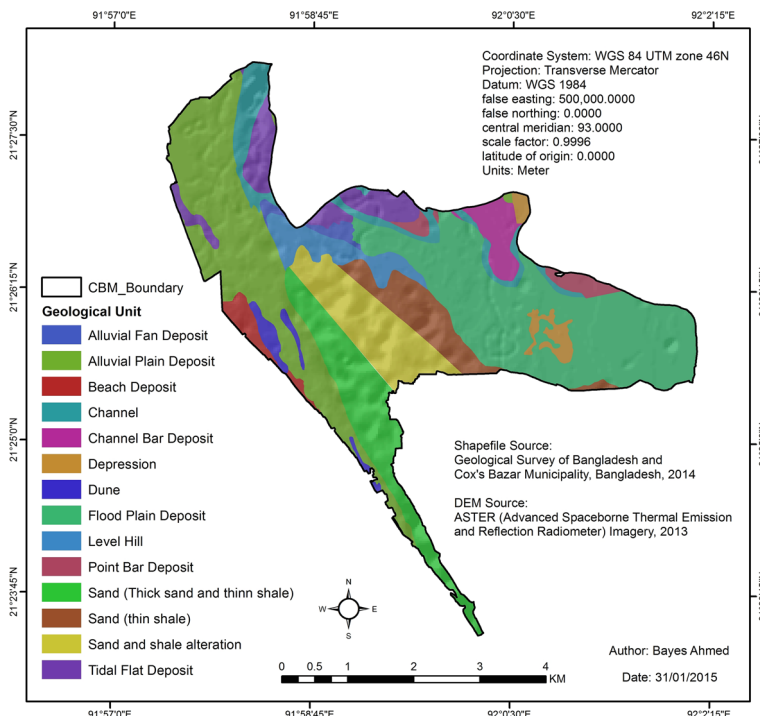


**Fig. 14** Geological map of CBM

factor weights for AHP and WLC were assigned using the PRA maps. The CR of AHP method was found <0.1 that can be considered as acceptable (Saaty 1977). The LSM derived from AHP method is illustrated in Fig. 20.

In case of WLC method, the procedure is simple. For each factor map, a weight was assigned (Table 5), and the total factor weight sum was 1. In WLC, first the factor maps multiplied the weights, and all the weighted factor maps were then aggregated (Fig. 21).

## 6.2 Logistic regression results

For LR analysis, the Boolean landslide inventory map (Fig. 6) was considered as dependent variable, and the 12 factors maps (Figs. 2d, 7b, 8, 9, 10, 11, 12, 13, 14, 15, 16, 17) were taken into account as independent variables (with 25 % thresholds). The regression equation is found as follows (Eq. 8):

$$\begin{aligned}
 \text{logit (landslides)} = & -144.8048 - 0.284121 \times \text{SR} - 0.756613 \times \text{DR} \\
 & - 0.529084 \times \text{FA} + 0.486189 \times \text{GE} + 1.776796 \times \text{GM} \\
 & - 0.030485 \times \text{LC} + 17.448088 \times \text{NV} - 1.465677 \times \text{PR} \\
 & + 0.159403 \times \text{RO} + 0.287524 \times \text{SL} + 17.452729 \times \text{SM} \\
 & + 0.306172 \times \text{ST}
 \end{aligned} \tag{8}$$

The regression statistics is calculated as follows:

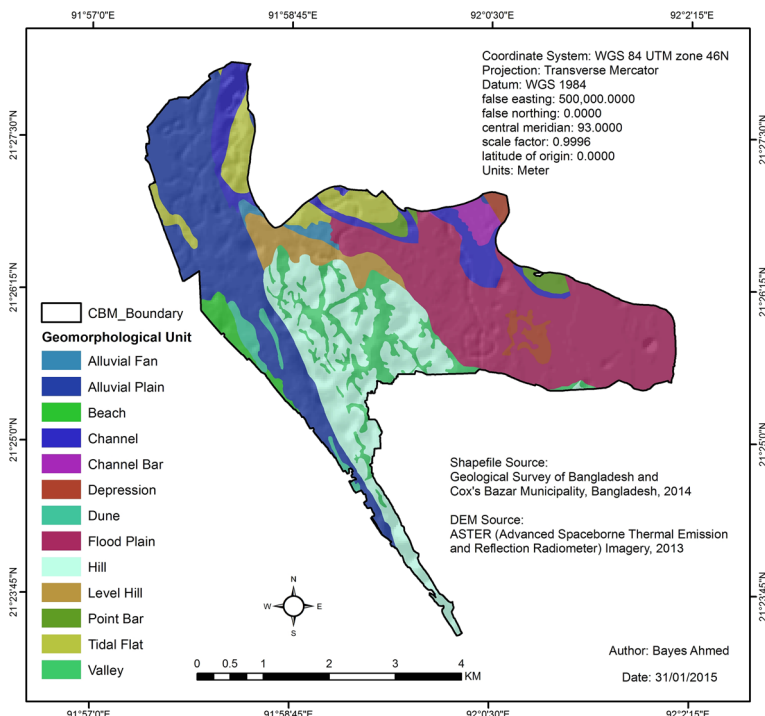


**Fig. 15** Geomorphological map

Number of total observations = 77,720 (number of cells)  
 Number of 0 s in study area = 77,646 (here, 0 = no landslide)  
 Number of 1 s in study area = 74 (here, 1 = the landslide location)  
 Percentage of 0 s in study area = 99.9048; percentage of 1 s in study area = 0.0952  
 Number of auto-sampled observations = 7524  
 Number of 0 s in sampled area = 7515; number of 1 s in sampled area = 9  
 Percentage of 0 s in sampled area = 99.8804, percentage of 1 s in sampled area = 0.1196  
 $-2 \log L_0 = 139.1045$ , and  $-2 \log(\text{Likelihood}) = 75.9240$ ; and pseudo  $R_{\text{square}} = 0.4542$

The ‘Pseudo  $R_{\text{square}}$ ’ is found  $>0.2$  that is considered as a good fit (Eastman 2012). The LR-generated LSM map is depicted in Fig. 22.

It is noticeable that soil moisture is calculated as the most effective factor ( $B = +17.452729$ ), and precipitation ( $B = -1.465677$ ) as the least effective variable (Eq. 8).

### 6.3 Multiple logistic regression results

The landslide inventory map was undertaken as dependent, and the factor maps were considered as dependent variables for MLR analysis. The MLR equation is found as follows (Eq. 9):

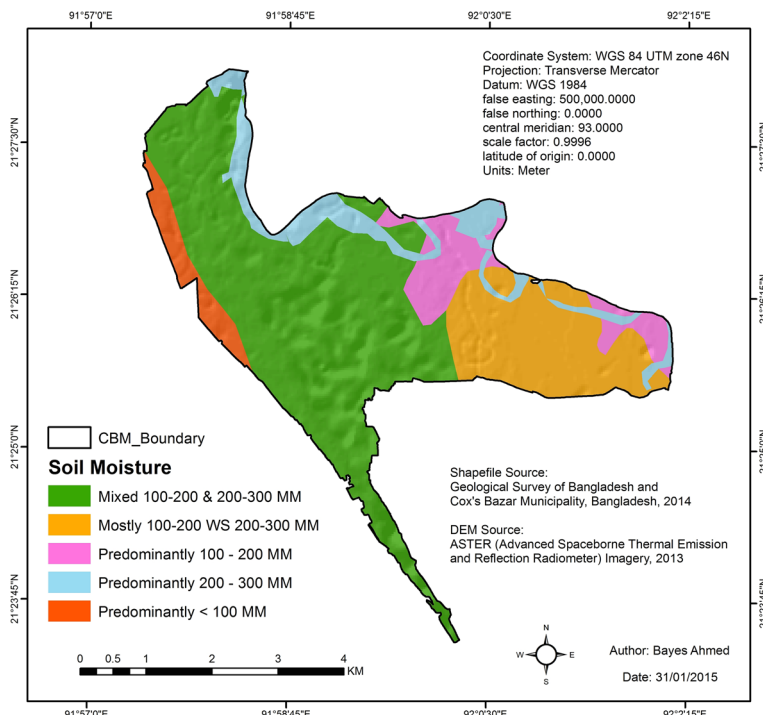


**Fig. 16** Soil moisture map

$$\begin{aligned}
 \text{Landslides} = & -0.0098 + 0.0003 \times \text{SR} - 0.0004 \times \text{DR} \\
 & - 0.0003 \times \text{FA} + 0.0002 \times \text{GL} + 0.0031 \times \text{GM} \\
 & - 0.0005 \times \text{LC} + 0.0012 \times \text{NV} + 0.0012 \times \text{PR} \\
 & - 0.0003 \times \text{RO} + 0.0017 \times \text{SL} - 0.0001 \times \text{SM} \\
 & + 0.0005 \times \text{ST}
 \end{aligned} \tag{9}$$

For analysing the significance of the overall regression,  $F$  test and for single variable or intercept,  $T$  test was performed. The two-tailed hypothesis tests assumed the significance level,  $\alpha = 0.05$ , where  $p < 0.05$  defines significance. The apparent (0.098232) and adjusted (0.095800)  $R$ , and the apparent (0.009650) and adjusted (0.009178)  $R$  square values were found low. The  $F(12, 23081)$  was found 18.741064. Moreover, the P values for the regression and residual were calculated  $<0.05$  (Table 6). It proves that the overall MLR (Eq. 9) is statistically significant.

In the next stage, attempt was made to test the significance of the individual MLR coefficients. The  $p$  values of GM, SL, NV, and PR were found most significant (Table 7). The LSM using MLR is depicted in Fig. 23.

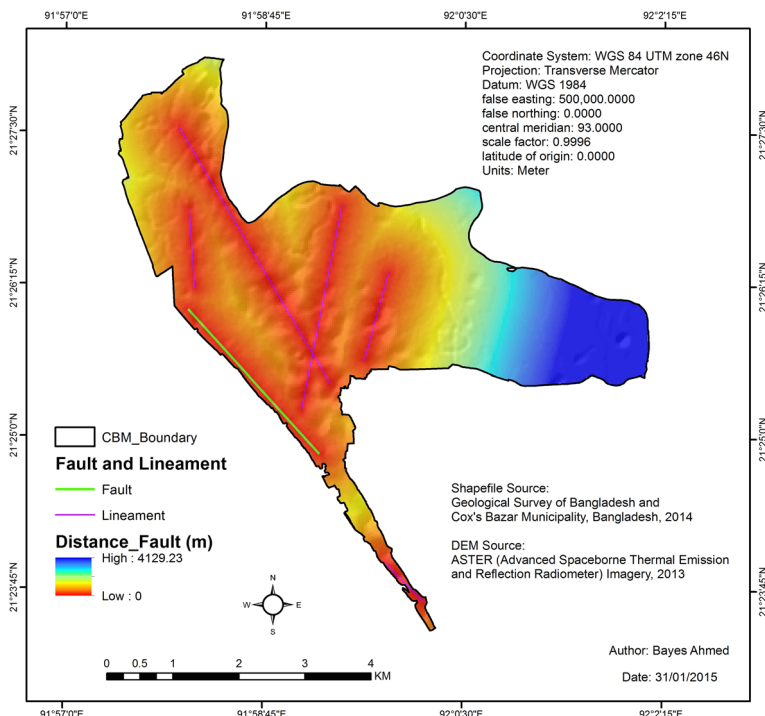


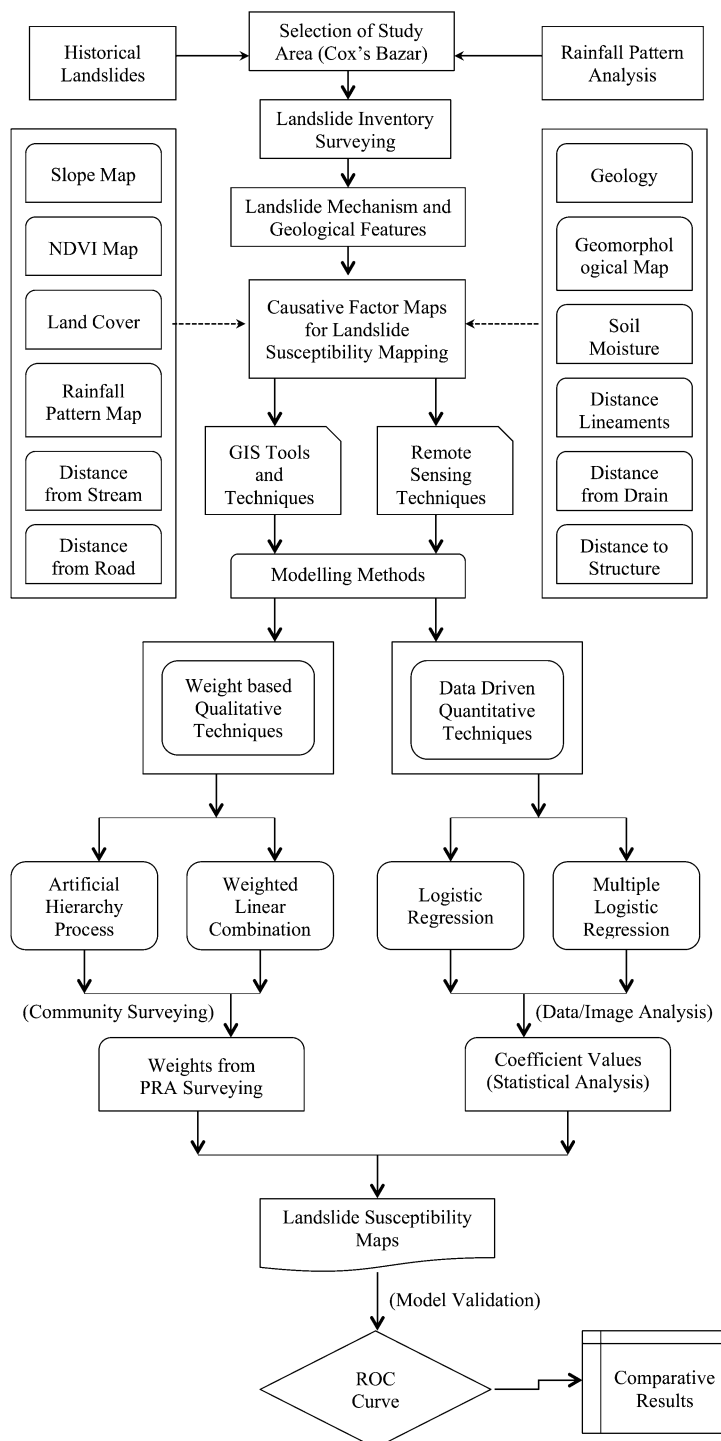
**Fig. 17** Distance from fault and lineaments

## 7 Validation of the models

To determine the statistical reliability of the results, the area under the relative operating characteristic (ROC) curve (AUC), or simply AUC method was employed. The AUC is a good indicator to evaluate the performance of a model qualitatively, and it is being widely used for LSM validation (Kavzoglu et al. 2014; Poudyal et al. 2010; Ahmed 2014). AUC values  $\leq 0.5$  indicate no improvement, between 0.7 and 0.9 indicate reasonable agreement, and AUC  $\geq 0.9$  represents ideal situation (Pontius and Schneider 2001; Eastman 2012).

Figure 24 shows the calculated AUC values (using equal interval, thresholds of 25 and 10 % stratified random samples) for LSM, indicating the accuracy of the models implemented. AUC values of AHP, WLC, LR, and MLR were calculated as 0.889, 0.859, 0.749, and 0.904, respectively, indicating acceptable level of performance. It can be concluded that only MLR-generated LSM is found to be ideal in terms of the model validation results (Fig. 24).

Now a comparative analysis is conducted to identify the similarities or differences found in different parts of Bangladesh and neighbouring countries based on other researchers works. Table 8 shows the accuracy results found by different authors who implemented AHP, WLC, LR, and MLR methods for LSM. The model validation accuracies were found between 74 and 94 % (Table 8) by them. On the other hand, the validation accuracies are calculated between 74 and 90 % for this article, which is quite

**Fig. 18** Flow chart of methodology

**Table 4** Pairwise comparison matrix for AHP

Pairwise comparison 9 point continuous rating scale											Eigen values		
Factor maps	1/9		1/7		1/5		1/3		1		Eigen values		
	Less important					Equal		More important					
	DR	FA	GL	GM	LC	NV	PR	RO	SL	SM	ST	SR	
DR	1											0.0227	
FA	1/3	1										0.0135	
GL	7	8	1									0.1961	
GM	7	8	1	1								0.1961	
LC	6	7	1/5	1/5	1							0.0990	
NV	5	6	1/6	1/6	1/3	1						0.0661	
PR	2	3	1/5	1/5	1/3	1/2	1					0.0422	
RO	3	4	1/6	1/6	1/4	1/2	2	1				0.0436	
SL	5	6	3	3	4	5	6	7	1			0.2436	
SM	2	3	1/7	1/7	1/6	1/5	1/4	1/3	1/5	1		0.0256	
ST	2	5	1/7	1/7	1/5	1/4	1/3	1/2	1/5	1	1	0.0289	
SR	1/2	3	1/7	1/7	1/3	1/3	1/2	1/2	1/5	1/2	1/2	1	0.0226

Consistency ratio = 0.09 (acceptable)

DR = distance from drainage network, FA = distance from fault and lineaments, GL = geological unit, GM = geomorphological unit, LC = land cover type, NV = NDVI, PR = precipitation, RO = distance from road network, SL = slope, SM = soil moisture, ST = distance from stream network, and SR = distance from existing structure

similar to other researchers works. Therefore, it can be stated that the results achieved in this research work are acceptable, and scientifically represent the previous works.

## 8 Discussions and future research

The AHP, and WLC methods used weights assigned by the researcher. Different weights can produce susceptibility maps with different intensities. Therefore, the LSM outputs based on weight-based MCE techniques depend largely on the expert's knowledge on the specific context. This is a trial and error process. Assigning more weights to less triggering factors or vice versa can generate abrupt results. Moreover, there is no recognized convention on assigning weights for the factor maps. In general, the experts or researchers choose the factor weights based on theoretical knowledge. But the weights should be selected after proper discussions with the local people, relevant officials, and stakeholders. It means both the empirical and theoretical expertise is recommended. It is possible to achieve higher AUC values from AHP and WLC methods using different weights. But this does not prove that the results are accurate and represent the real-world scenario or the local context. Resolving the issues related to assigning weights can be subject to future research.

Again, the data-driven statistical techniques, like the regression analyses, can also give abrupt results. The positive value of the regression coefficients indicates positive relation with landslide occurrence and vice versa (Kavzoglu et al. 2014). An independent variable

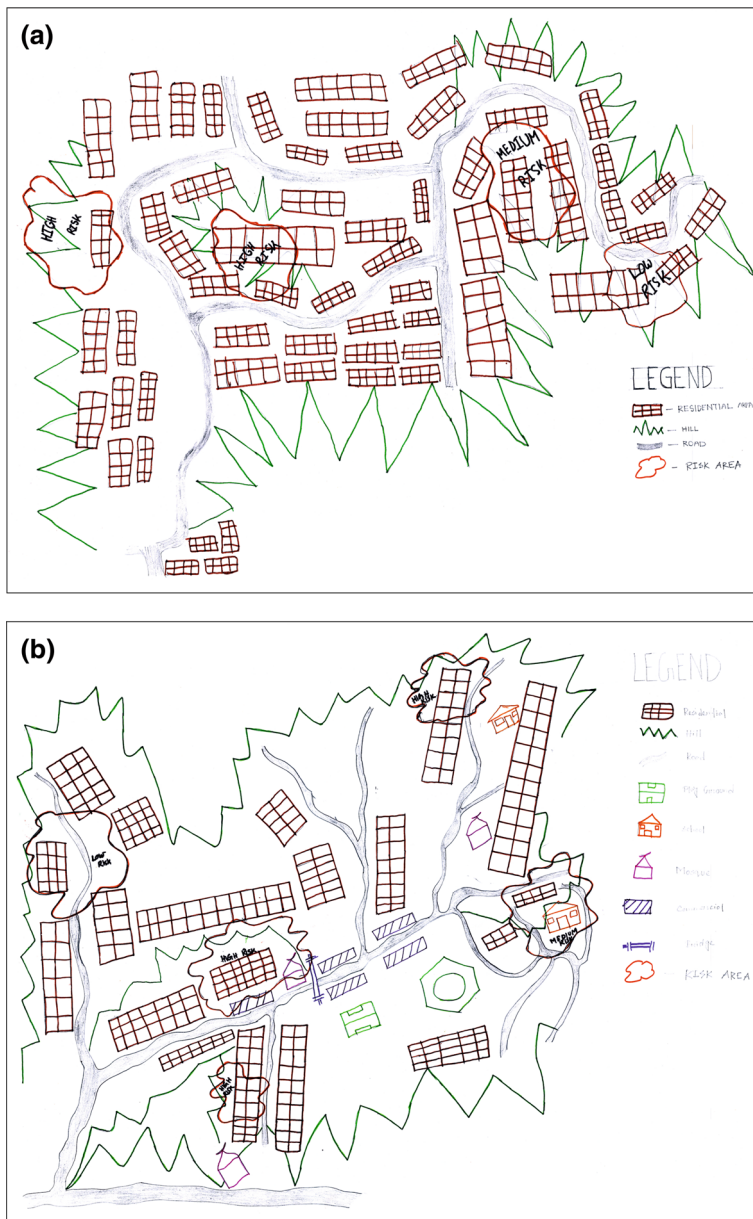


**Fig. 19** Vulnerability maps of **a** *Badshahghona*, and **b** *Lighthouse Para* communities in CBM using PRA techniques. *Source:* Bayes Ahmed, Fieldwork, September–October 2014

with a positive and higher coefficient value represents that it can increase the probability of landslides than the other variables. From the binomial LR analysis, it is found that the higher the soil moisture ( $B = +17.452729$ ) and NDVI ( $B = +17.448088$ ) value, the higher the likelihood of a landslide will be occurring (Eq. 8). On the other hand, the MLR analysis results indicate that the geomorphology, NDVI, precipitation, and slope values

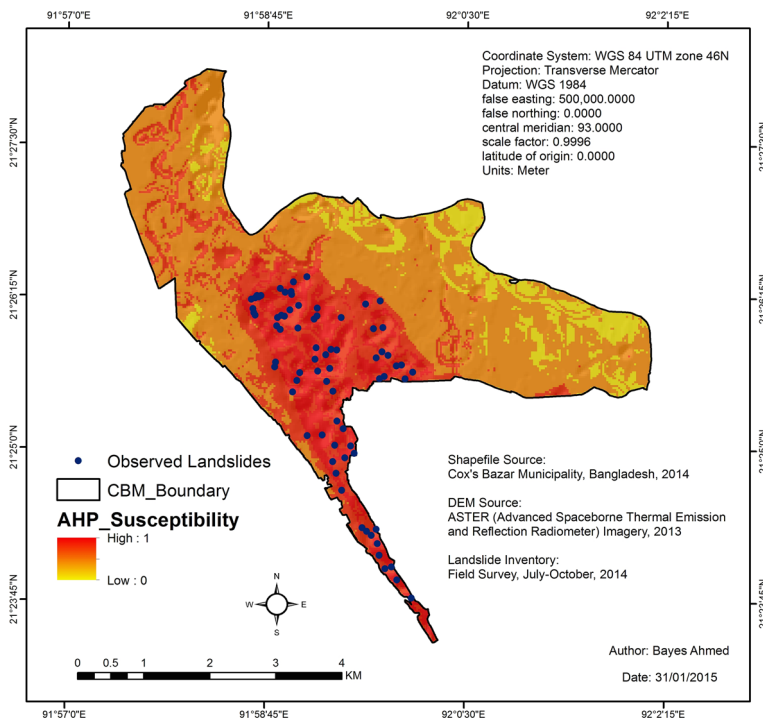


**Fig. 20** Landslide susceptibility map derived from AHP method

**Table 5** Factor weights for WLC analysis

Factors	DR	FA	GL	GM	LC	NV	PR	RO	SL	SM	ST	SR
Weight	0.05	0.02	0.15	0.15	0.10	0.10	0.07	0.03	0.20	0.05	0.03	0.05

increase the landslide likelihood (Eq. 9). Therefore, it can be concluded that the different LR methods are showing different results and accuracies. This could be a topic for future research.

In this research, Landsat satellite images and ASTER DEM were used for analysis. For better accuracy, higher-resolution images can be used. Moreover, the quality and resolution of the historical base maps were not good enough for accuracy assessment. Some of the factor maps (e.g. road, drain, structure) were collected from CBM. The physical feature surveying of those maps were not up to date. These were the drawbacks related to data collection. This research is not assuring that the LSMs produced using different techniques are applicable for real-world case studies. These LSMs are simply generating the idea that it is possible to produce statistically feasible LSMs using the available data sets and techniques. If the limitations can be minimized and better factor maps can be incorporated, then higher accuracy is expected. Future research should also emphasize on developing a reliable, free, and publicly accessible landslide early-warning system for the vulnerable communities (BUET-JIDPUS 2015).

In general, a disaster risk is the product of hazard and vulnerability. The casualties and damages from a disaster can be determined by human culture, society's response

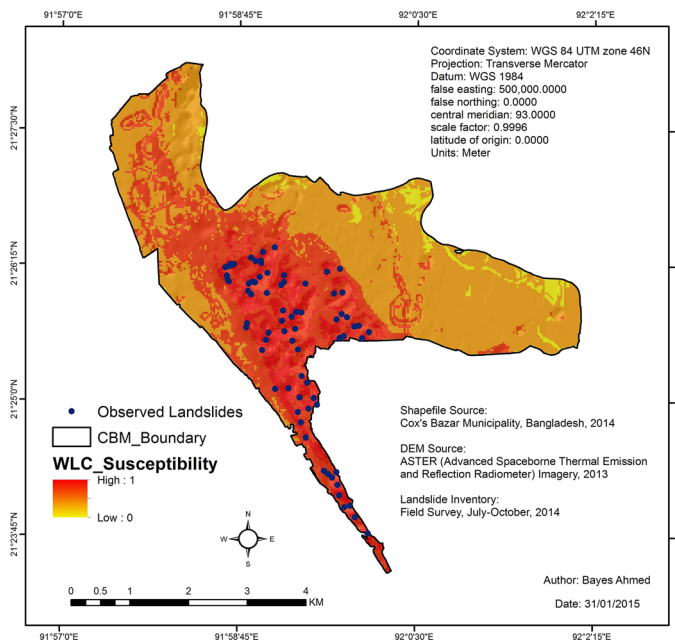


**Fig. 21** Landslide susceptibility map derived from WLC method

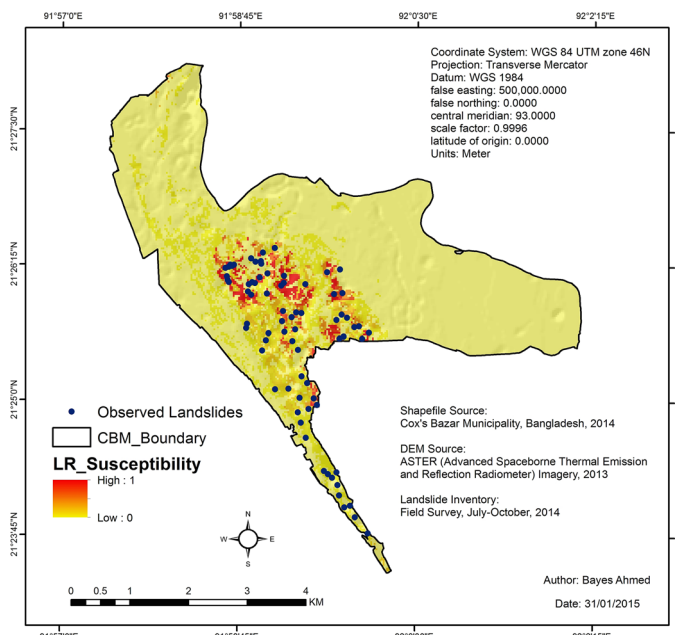


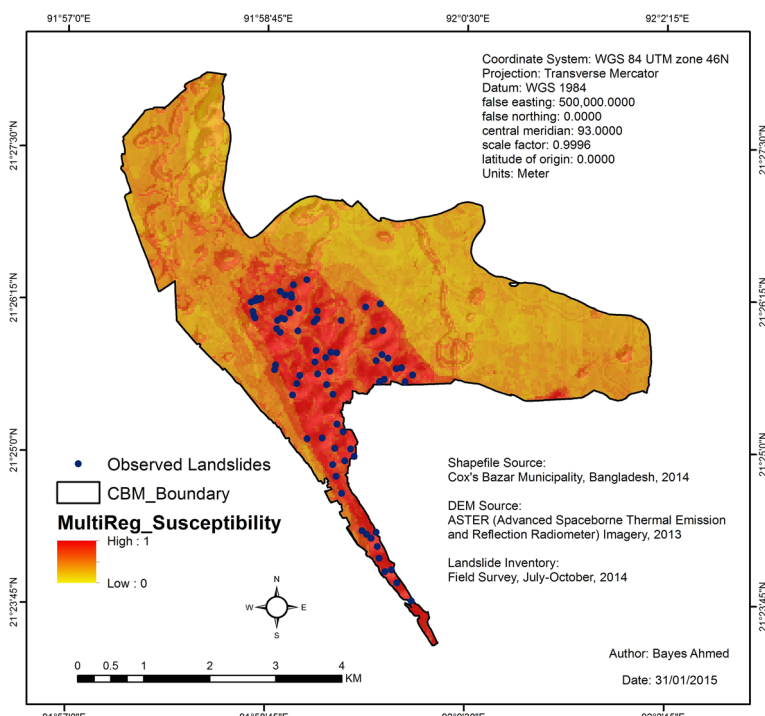
**Fig. 22** Landslide susceptibility map derived from LR method

**Table 6** ANOVA regression table for *F* test

Model	Apparent degrees of freedom ( <i>df</i> )	Sum of squares	Mean square	<i>P</i> value
Regression	12	0.71	0.06	<0.0001
Residual	23,081	73.05	0.0031	
Total	23,093	73.76		

**Table 7** *T* test (23,081) results for the individual MLR coefficients

Source	Coefficient	<i>T</i> -score	<i>P</i> value
Intercept	−0.009796	−3.687570	0.000227
SR	0.000323	0.519310	0.603557
DR	−0.000382	−0.593147	0.553187
FA	−0.000323	−0.464431	0.642652
GL	0.000155	0.204514	0.837965
GM	0.003138	3.845105	0.000121
LC	−0.000472	−1.155446	0.248102
NV	0.001166	2.715143	0.006631
PR	0.001207	2.113777	0.034552
RO	−0.000324	−0.577751	0.563945
SL	0.001685	5.341352	0.000010
SM	−0.000120	−0.228407	0.819648
ST	0.000539	1.357928	0.174509

**Fig. 23** Landslide susceptibility map derived from MLR model

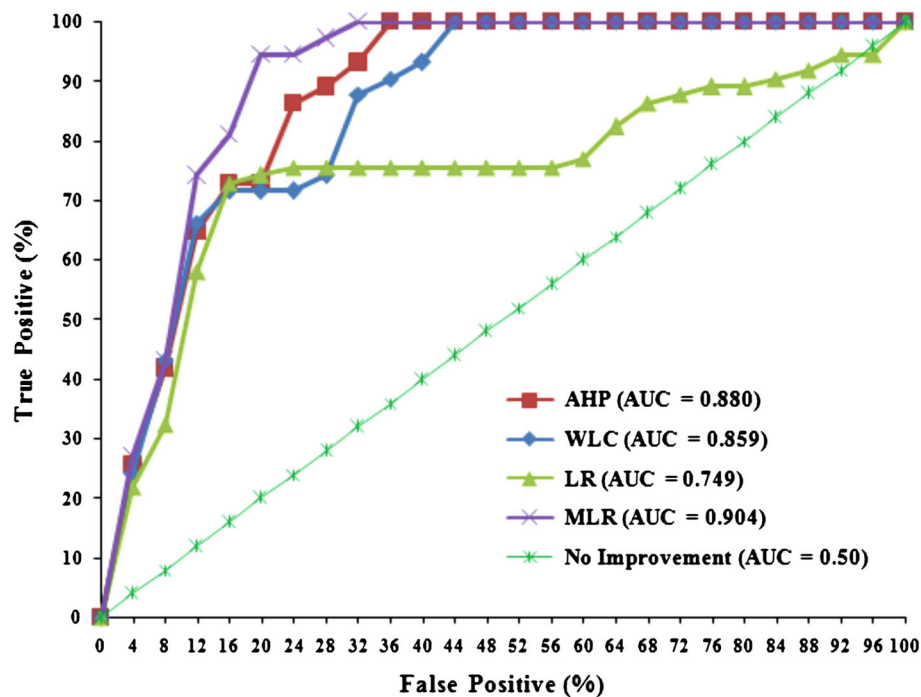


**Fig. 24** Assessment of the model performances based on the ROC curves

**Table 8** Comparison of model validation accuracies

Author (year)	Study area (country)	Validation accuracy (%)			
		AHP	WLC	LR	MLR
Devkota et al. (2013)	Nepal	–	–	89	–
Shahabi and Hashim (2015)	Malaysia	91	89	–	–
Ramani et al. (2011)	India	–	–	85	–
Ahmed (2014)	Bangladesh	90	91	–	–
Park et al. (2013)	Korea	79	–	80	–
Ahmed and Rubel (2013)	Bangladesh	–	89	–	97
Lee and Sambath (2006)	Cambodia	–	–	86	–
Kavzoglu et al. (2014)	Turkey	94	–	91	–
Felicísimo et al. (2013)	Spain	–	–	–	76
Shahabi et al. (2013)	Iran	–	–	88	74

to the impact of extreme geophysical events, and the forces of socio-economic changes (Alexander 2000: 250). Moreover, analyses related to GIS/RS-based landslide hazard zoning are defined as inductive method that is less efficient, based on weaker initial assumptions, and do not depict the overall scenario (Alexander 2008). It is also argued that research focusing on landslide hazards and physical mechanisms of slope failure have already been conducted extensively. On the other hand, GIS/RS or the computer-assisted techniques have failed to identify the role of vulnerability in

determining landslide risks (Alexander 2006). Therefore, future research should focus more on landslide vulnerability, people's perception, cultural and historical aspects, indigenous knowledge sharing, and institutional decision-making process (Alexander 2007; IFRC 2014). This can be achieved by incorporating a holistic approach to landslide disaster risk assessment, which should consider physical, ecological, social, economic, cultural, and institutional aspects of landslide vulnerability (Birkmann et al. 2013).

## 9 Conclusion

Landslides are poly-causal phenomena causing devastating casualties, economic loss, and damages to properties. Moreover, globally the impact of landslides is increasing gradually. Petley et al. (2005) already argued that majority of human fatalities and costs associated with landslide disasters occur in economically least-developed countries. This scenario is true for the urbanized hilly areas of CBM. The aim of this article is to prepare statistically valid and reasonable landslide susceptibility maps, using the freely available data sets, for the people living in the dangerous hilly slopes in CBM. To achieve this goal, GIS- and RS-based modelling techniques were implemented. These are two weight-based MCE methods (i.e. AHP, and WLC), and two data-driven statistical models (i.e. LR, and MLR). The landslide inventory map was then compared with the LSMs. The performances of the methods were validated using the ROC curves. The AUC values for AHP, WLC, LR, and MLR were calculated as 0.880, 0.859, 0.749, and 0.904, respectively. The MLR model is found statistically significant and representing the ideal situation. The availability of higher-resolution satellite images, better base maps, and up to date data sets can help producing better accuracies and validation results.

The current trend of landslide hazard mapping is associated with computer-assisted GIS and RS techniques. This kind of inductive technique neglects the views and vulnerability perception of the local people living with landslide risks. Therefore, the urban planners, scientists, and researchers should focus more on incorporating local, cultural, and indigenous knowledge through community-based participatory hazard mapping. It is also important to produce administrative hazard maps by consultation with the concerned experts and stakeholders. A comparative analysis by identifying the anomalies among the three different hazard maps (i.e. computer assisted, community, and expert opinion based) could be interesting for future research.

The landslide susceptibility maps as prepared in this research can be useful for hazard assessment and developing an early-warning system. The concerned decision makers, urban planners, engineers, and authorities of Cox's Bazar, Bangladesh, will find the outcome of this article interesting for real-life implementation. The results from LSMs will also be helpful for identifying the root causes of landslides, the most hazardous zones, and thus by taking necessary preparedness steps and reducing the landslide disaster risks in CBM.

**Acknowledgments** Bayes Ahmed is a Commonwealth Scholar funded by the UK govt. The author would like to thank the UCL Institute for Risk and Disaster Reduction (IRDR) for partially funding the fieldwork in Cox's Bazar Municipality (CBM), Bangladesh. The author is grateful to Professor Dr. David E. Alexander, Renato Forte, the local people, the relevant officials and experts from CBM. My special gratitude goes to the research assistants (Abdullah Al Nyem, Sourav Biswas, Kawser Uddin, Md. Ahsan Habib, Shorajit Biswas, Shoukat Ahmed, and K.M. Risaduzzaman) from the Department of Urban and Regional Planning, Chittagong University of Engineering and Technology (CUET), Bangladesh. Finally, the author wants to thank

the editors and the reviewers of ‘Natural Hazards’ journal for their constructive comments that improved the quality of this manuscript.

## References

- Agresti A (2007) An introduction to categorical data analysis (Chapter 4), 2nd edn. Wiley, Hoboken
- Ahmed B (2011) Urban land cover change detection analysis and modeling spatio-temporal growth dynamics using remote sensing and GIS techniques: a case study of Dhaka, Bangladesh. Masters Dissertation. University of New Lisbon (UNL), Lisbon, Portugal
- Ahmed B (2014) Landslide susceptibility mapping using multi-criteria evaluation techniques in Chittagong Metropolitan Area, Bangladesh. *Landslides*. doi:[10.1007/s10346-014-0521-x](https://doi.org/10.1007/s10346-014-0521-x)
- Ahmed B, Ahmed R (2012) Modeling urban land cover growth dynamics using multi-temporal satellite images: a case study of Dhaka, Bangladesh. *ISPRS Int J Geo-Inf* 1(1):3–31
- Ahmed B, Rubel YA (2013) Understanding the issues involved in urban landslide vulnerability in Chittagong Metropolitan Area, Bangladesh. Association of American Geographers (AAG), Washington
- Ahmed B, Ahmed R, Zhu X (2013a) Evaluation of model validation techniques in land cover dynamics. *ISPRS Int J Geo-Inf* 2(3):577–597
- Ahmed B, Kamruzzaman M, Zhu X, Rahman M, Choi K (2013b) Simulating land cover changes and their impacts on land surface temperature in Dhaka, Bangladesh. *Remote Sens* 5(11):5969–5998
- Ahmed B, Rahman MS, Rahman S, Huq FF, Ara S (2014) Landslide inventory report of Chittagong Metropolitan Area, Bangladesh. BUET-Japan Institute of Disaster Prevention and Urban Safety (BUET-JIDPUS); Bangladesh University of Engineering and Technology (BUET), Dhaka-1000, Bangladesh. <http://www.landslidebd.com/reports/>. Accessed on 23 June 2015
- Akgun A (2012) A comparison of landslide susceptibility maps produced by logistic regression, multi-criteria decision, and likelihood ratio methods: a case study at Izmir, Turkey. *Landslides* 9:93–106
- Alexander D (1991) Information technology in real-time for monitoring and managing natural disasters. *Prog Phys Geogr* 15:238. doi:[10.1177/03091339101500302](https://doi.org/10.1177/03091339101500302)
- Alexander DE (2000) Confronting catastrophe: new perspective on natural disasters (Chapter 9), 1st edn. Terra Publishing, Hertfordshire
- Alexander DE (2004). Vulnerability to landslides. In: Glade T, Anderson M, Crozier MJ (eds) *Landslide hazard and risk*. Wiley, New York. doi:[10.1002/9780470012659](https://doi.org/10.1002/9780470012659)
- Alexander D (2006) Globalization of disaster: trends, problems and dilemmas. *J Int Aff* 59(2):1–22
- Alexander D (2007) Making research on geological hazards relevant to stakeholders’ needs. *Quatern Int* 171–172:186–192
- Alexander DE (2008) A brief survey of GIS in mass-movement studies, with reflections on theory and methods. *Geomorphology* 94:261–267
- Alexander DE (2014) Assessing vulnerability in Europe and the world. In: Birkmann J (ed) *Assessment of vulnerability to natural hazards: a European perspective*. Elsevier, San Diego
- ArcGIS® 10.2 Help (2014) Environmental systems research institute (ESRI). Redlands, CA, USA. <http://resources.arcgis.com/en/help/main/10.2/>. Accessed 12 February 2015
- Armaş A (2012) Weights of evidence method for landslide susceptibility mapping Prahova Subcarpathians, Romania. *Nat Hazards* 60(3):937–950
- Ayalew L, Yamagishi H (2005) The application of GIS-based logistic regression for landslide susceptibility mapping in the Kakuda-Yahiko Mountains, Central Japan. *Geomorphology* 65:15–31. doi:[10.1016/j.geomorph.2004.06.010](https://doi.org/10.1016/j.geomorph.2004.06.010)
- Aydi A, Zairi M, Dhia HB (2013) Minimization of environmental risk of landfill site using fuzzy logic, analytical hierarchy process, and weighted linear combination methodology in a geographic information system environment. *Environ Earth Sci* 68:1375–1389. doi:[10.1007/s12665-012-1836-3](https://doi.org/10.1007/s12665-012-1836-3)
- Ballabio C, Sterlacchini S (2012) Support vector machines for landslide susceptibility mapping: the Staffora River basin case study, Italy. *Math Geosci* 44(1):47–70
- BBS (2013) District statistics 2011: Cox’s Bazar. Bangladesh Bureau of Statistics (BBS), Statistics and Informatics Division (SID), Ministry of Planning, Dhaka, Government of the People’s Republic of Bangladesh
- Birkmann J (ed) (2006) Measuring vulnerability to natural hazards: towards disaster resilient societies, 1st edn. United Nations University Press, Tokyo
- Birkmann J, Cardona OD, Carreno ML, Barbat AH, Pelling M, Schneiderbauer S, Kienberger S, Keiler M, Alexander D, Zeil P, Welle T (2013) Framing vulnerability, risk and societal responses: the MOVE framework. *Nat Hazards* 67:193–211. doi:[10.1007/s11069-013-0558-5](https://doi.org/10.1007/s11069-013-0558-5)

- BUET-JIDPUS (2015) Developing dynamic web-GIS based early warning system for the communities at landslide risks in Chittagong Metropolitan Area, Bangladesh. BUET-Japan Institute of Disaster Prevention and Urban Safety (BUET-JIDPUS); Bangladesh University of Engineering and Technology (BUET), Dhaka-1000, Bangladesh. <http://www.landslidebd.com/warning-system/>. Accessed on 24 June 2015
- CDMP-II (2012) Comprehensive disaster management programme-II (CDMP-II). Landslide inventory and land-use mapping, DEM preparation, precipitation threshold value and establishment of early warning devices. Ministry of Food and Disaster Management, Disaster Management and Relief Division, Government of the People's Republic of Bangladesh
- Couture R (2011) Landslide terminology—national technical guidelines and best practices on landslides. Geological survey of Canada, Open file 6824, 12 p
- Cruden DM (1991) A simple definition of landslide. Bull Int As Eng Geol 43:27–29
- Dai FC, Lee CF (2002) Landslide characteristics and slope instability modeling using GIS, Lantau Island, Hong Kong. Geomorphology 42(3–4):213–228
- Devkota KC, Regmi AD, Pourghasemi HR, Yoshida K, Pradhan B, Ryu IC, Dhalal MR, Althuwaynee OF (2013) Landslide susceptibility mapping using certainty factor, index of entropy and logistic regression models in GIS and their comparison at Mugling–Narayanghat road section in Nepal Himalaya. Nat Hazards 65:135–165. doi:[10.1007/s11069-012-0347-6](https://doi.org/10.1007/s11069-012-0347-6)
- Eastman R (2012) IDRISI Selva help system. Clark Labs, Clark University, Worcester
- Feizizadeh B, Blaschke T (2013) GIS-multicriteria decision analysis for landslide susceptibility mapping: comparing three methods for the Urmialake basin, Iran. Nat Hazards 65:2105–2128. doi:[10.1007/s11069-012-0463-3](https://doi.org/10.1007/s11069-012-0463-3)
- Felicísimo Á, Cuartero A, Remondo J, Quirós E (2013) Mapping landslide susceptibility with logistic regression, multiple adaptive regression splines, classification and regression trees, and maximum entropy methods: a comparative study. Landslides 10:175–189. doi:[10.1007/s10346-012-0320-1](https://doi.org/10.1007/s10346-012-0320-1)
- Guzzetti F, Carrara A, Cardinali M, Reichenbach P (1999) Landslide hazard evaluation: a review of current techniques and their application in a multi-scale study, Central Italy. Geomorphology 31:181–216
- Hossain, M. (2012). Cox's Bazar. In: Islam N (ed) Banglapedia, national encyclopaedia of Bangladesh, 2nd edn. Banglapedia Trust, Asiatic Society of Bangladesh, Dhaka, Bangladesh. [http://www.banglapedia.org/HT/C\\_0432.htm](http://www.banglapedia.org/HT/C_0432.htm). Accessed on 05 Feb 2015
- ICIMOD (2015) International efforts to identify post-quake hazards. International Centre for Integrated Mountain Development (ICIMOD), Kathmandu, Nepal. <http://www.icimod.org/?q=18072>. Accessed 23 June 2015
- IFRC (2014) World disasters report 2014—focus on culture and risk. International Federation of Red Cross and Red Crescent Societies (IFRC), Geneva, Switzerland. <http://www.ifrc.org/en/publications-and-reports/world-disasters-report/world-disasters-report-2013/>. Accessed on 24 June 2015
- Kavzoglu T, Sahin EK, Colkesen I (2014) Landslide susceptibility mapping using GIS-based multi-criteria decision analysis, support vector machines, and logistic regression. Landslides 11:425–439. doi:[10.1007/s10346-013-0391-7](https://doi.org/10.1007/s10346-013-0391-7)
- Kayastha P, Dhalal MR, Smedt FD (2012) Landslide susceptibility mapping using the weight of evidence method in the Tinau watershed, Nepal. Nat Hazards 63:479–498. doi:[10.1007/s11069-012-0163-z](https://doi.org/10.1007/s11069-012-0163-z)
- Kayastha P, Bijukchhen S, Dhalal M, Smedt F (2013) GIS based landslide susceptibility mapping using a fuzzy logic approach: a case study from Ghurmi–Dhad Khola area, Eastern Nepal. J Geol Soc India 82(3):249–261
- Khamehchian M, Abdolmaleki P, Rakei B (2011) Landslide susceptibility mapping using back propagation neural networks and logistic regression: the Sephidargole case study, Semnan, Iran. Geomech Geoeng 6(3):237–250
- Lee S (2004) Application of likelihood ratio and logistic regression models to landslide susceptibility mapping using GIS. Environ Manag 34(2):223–232
- Lee S, Lee ML (2006) Detecting landslide location using KOMPSAT 1 and its application to landslide-susceptibility mapping at the Gangneung area, Korea. Adv Space Res 38:2261–2271
- Lee S, Sambath T (2006) Landslide susceptibility mapping in the Damrei Romel area, Cambodia using frequency ratio and logistic regression models. Environ Geol 50:847–855. doi:[10.1007/s00254-006-0256-7](https://doi.org/10.1007/s00254-006-0256-7)
- Li C, Ma T, Sun L, Li W, Zheng A (2012) Application and verification of a fractal approach to landslide susceptibility mapping. Nat Hazards 61(1):169–185
- Malczewski J (2004) GIS-based land-use suitability analysis: a critical overview. Prog Plan 62:3–65
- Oh HJ, Pradhan B (2011) Application of a neuro-fuzzy model to landslide-susceptibility mapping for shallow landslides in a tropical hilly area. Comput Geosci 37(9):1264–1276

- Ohlmacher GC, Davis JC (2003) Using multiple logistic regression and GIS technology to predict landslide hazard in northeast Kansas, USA. *Eng Geol* 69:331–343. doi:[10.1016/S0013-7952\(03\)00069-3](https://doi.org/10.1016/S0013-7952(03)00069-3)
- Park S, Choi C, Kim B, Kim J (2013) Landslide susceptibility mapping using frequency ratio, analytic hierarchy process, logistic regression, and artificial neural network methods at the Inje area, Korea. *Environ Earth Sci* 68:1443–1464. doi:[10.1007/s12665-012-1842-5](https://doi.org/10.1007/s12665-012-1842-5)
- Pellicani R, Western CJV, Spilotro G (2013) Assessing landslide exposure in areas with limited landslide information. *Landslides*. doi:[10.1007/s10346-013-0386-4](https://doi.org/10.1007/s10346-013-0386-4)
- Petley DN, Dunning SA, Rosser NJ (2005) The analysis of global landslide risk through the creation of a database of worldwide landslide fatalities. In: Hungr O, Fell R, Couture R, Eberhardt E (eds) *Landslide risk management*. AT Balkema, Amsterdam, pp 367–374
- Pontius RG Jr, Schneider L (2001) Land-use change model validation by a ROC method for the Ipswich watershed, Massachusetts, USA. *Agric Ecosyst Environ* 85(1–3):239–248
- Poudyal CP, Chang C, Oh HJ, Lee S (2010) Landslide susceptibility maps comparing frequency ratio and artificial neural networks: a case study from the Nepal Himalaya. *Environ Earth Sci* 61:1049–1064. doi:[10.1007/s12665-009-0426-5](https://doi.org/10.1007/s12665-009-0426-5)
- Pradhan B, Lee S, Buchroithner MF (2010) A GIS-based back-propagation neural network model and its cross-application and validation for landslide susceptibility analyses. *Comput Environ Urban Syst* 34(3):216–235
- Ramani SE, Pitchaimani K, Gnanamanickam VR (2011) GIS based landslide susceptibility mapping of Tevankarai Ar sub-watershed, Kodaikanal, India using binary logistic regression analysis. *J Mt Sci* 8:505–517
- Reis S, Yalcin A, Atasoy M, Nisanci R, Bayrak T, Erduran M, Sancar C, Ekercin S (2012) Remote sensing and GIS-based landslide susceptibility mapping using frequency ratio and analytical hierarchy methods in Rize province (NE Turkey). *Environ Earth Sci* 66:2063–2073. doi:[10.1007/s12665-011-1432-y](https://doi.org/10.1007/s12665-011-1432-y)
- Saaty TL (1977) A scaling method for priorities in hierarchical structures. *J Math Psychol* 15:231–281
- Sabokbar HF, Roodposhti MS, Tazik E (2014) Landslide susceptibility mapping using geographically-weighted principal component analysis. *Geomorphology* 226:15–24
- Sezer EA, Pradhan B, Gokceoglu C (2011) Manifestation of an adaptive neuro-fuzzy model on landslide susceptibility mapping: Klang valley, Malaysia. *Expert Syst Appl* 38(7):8208–8219
- Shahabi H, Hashim M (2015) Landslide susceptibility mapping using GIS-based statistical models and remote sensing data in tropical environment. *Sci Rep* 5:9899. doi:[10.1038/srep09899](https://doi.org/10.1038/srep09899)
- Shahabi H, Ahmad BB, Khezri S (2013) Evaluation and comparison of bivariate and multivariate statistical methods for landslide susceptibility mapping (case study: Zab basin). *Arab J Geosci* 6(10):3885–3907. doi:[10.1007/s12517-012-0650-2](https://doi.org/10.1007/s12517-012-0650-2)
- Sujatha E, Rajamanickam V (2011) Landslide susceptibility mapping of Tevankarai Ar sub-watershed, Kodaikanal, India, using weighted similar choice fuzzy model. *Nat Hazards* 59(1):401–425
- Tachikawa T, Hato M, Kaku M, Iwasaki A (2011) The characteristics of ASTER GDEM version 2, IGARSS. <http://www.jspacesystems.or.jp/ersdac/GDEM/E/1.html>. Accessed 12 Oct 2014
- Talaei R (2014) Landslide susceptibility zonation mapping using logistic regression and its validation in Hashtchin Region, Northwest of Iran. *J Geol Soc India* 84:68–86
- USGS (2014) Frequently asked questions about the landsat missions. Department of the Interior, U.S. Geological Survey (USGS). [http://landsat.usgs.gov/band\\_designations\\_landsat\\_satellites.php](http://landsat.usgs.gov/band_designations_landsat_satellites.php). Accessed 13 Feb 2015
- USGS (2015) USGS global visualization viewer. Department of the Interior, U.S. Geological Survey (USGS). <http://glovis.usgs.gov/index.shtml>. Accessed 10 Feb 2015
- Wisner B, Blaikie P, Cannon T, Davis I (2004) *At Risk: natural hazards, people's vulnerability and disasters*, 1st edn. Routledge, New York
- Yeon YK, Han JG, Ryu KH (2010) Landslide susceptibility mapping in Injae, Korea, using a decision tree. *Eng Geol* 116(3):274–283
- Yilmaz C, Topal T, Suzen M (2012) GIS-based landslide susceptibility mapping using bivariate statistical analysis in Devrek (Zonguldak-Turkey). *Environ Earth Sci* 65(7):2161–2178
- Zhang X, Yang F (2004). RClimDex (1.0): User manual. Climate Research Branch, Environment Canada, Downsview, Ontario, Canada